ORIGINAL ARTICLE

Optimal glycan density for interactions between Siglec-8 and sialyl sulfo oligosaccharides

Risa Naka[1] · Simon Sau Yin Law[2] · Ayaka Tateishi[2] · Keiji Numata [1,2,3] · Masashi Ohmae[1]

Abstract

Siglec-8, a lectin involved in the suppression of allergic responses, is considered a therapeutic target for developing glycan materials that enable the regulation of inflammatory diseases. In developing such glycan materials, the "multivalent effect" is essential for regulating immune responses. The "multivalent effect" dramatically increases the apparent affinities (avidities) of glycan-lectin interactions by clustering the glycan ligand multivalently. Numerous lectin-glycan interactions utilize this effect in immunological reactions, and Siglec-8 is thought to show an effect similar to those of other lectins. However, we hypothesized that increasing the local concentration of glycan ligands and modulating the glycan density are essential in allowing glycan ligands to interact effectively with Siglec-8. Here, we investigate the density-dependent changes in avidities between Siglec-8 and sialyl sulfo-oligosaccharides with a quartz crystal microbalance (QCM) for the first time. As a result, it was determined that Siglec-8 has an optimal glycan density ($\sim 9.2 \times 10^2$ molecules μm^{-2}) for preferred interactions. Additionally, this suggests that the regulation of glycan density is key to developing therapeutic materials targeting Siglec-8. The results described here will promote the development of glycan materials that ameliorate immune disorders such as inflammation and anaphylaxis.

Introduction

Sialic acid-binding immunoglobulin-like lectins (Siglecs) are expressed on the surfaces of immune cells to regulate their immune responses. Their unique property is recognition specificity toward sialic acid-containing glycan ligands

✉ Keiji Numata
   keiji.numata@riken.jp

✉ Masashi Ohmae
   ohmae.masashi.4n@kyoto-u.ac.jp

1   Department of Material Chemistry, Graduate School of Engineering, Kyoto University, Kyoto Daigaku Katsura, Nishikyo-ku, Kyoto 615-8510, Japan

2   Biomacromolecules Research Team, RIKEN Center for Sustainable Resource Science, 2-1 Hirosawa, Wako, Saitama 351-0198, Japan

3   Institute for Advanced Biosciences, Keio University, Nipponkoku 403-1, Daihouji, Tsuruoka, Yamagata 997-0017, Japan

[1]. Siglec-8, which is mainly expressed on eosinophils, mast cells and basophils, suppresses their activities through recognition of the sialylated glycan ligands and inhibits acute or chronic allergic diseases [2]. Thus, Siglec-8 is considered an important therapeutic target for regulating allergic responses, and the development of glycan materials that efficiently bind Siglec-8 is required to synthesize promising anti-inflammatory drugs.

To develop synthetic glycan materials that recruit Siglec-8 in the suppression of allergic reactions, two strategic steps need to be considered. The first is to develop ligands with high affinity (avidity) or even monovalency for Siglec-8 binding. Siglec-8 is known to recognize sialyl N-acetyllactosamine bearing a 6′-sulfate group [6′-su-SLacNAc; Neu5Ac$\alpha(2 \rightarrow 3)$Gal(6-SO$_3^-$)$\beta(1 \rightarrow 4)$GlcNAc], a terminal structure of sialylated keratan sulfate chains, as a glycan ligand [3, 4]. In addition, to allow the glycan ligands to match the concave pocket of Siglec-8, sialyl type II sulfo-hexasaccharides and pentasaccharides were recently developed, resulting in 2–7-fold increases in avidity toward Siglec-8 than sialyl type II sulfo-tetrasaccharides [5, 6]. Thus, glycan materials targeting Siglec-8 should be decorated with these sialylated keratan sulfate hexa- or pentasaccharides to increase their therapeutic efficiencies.
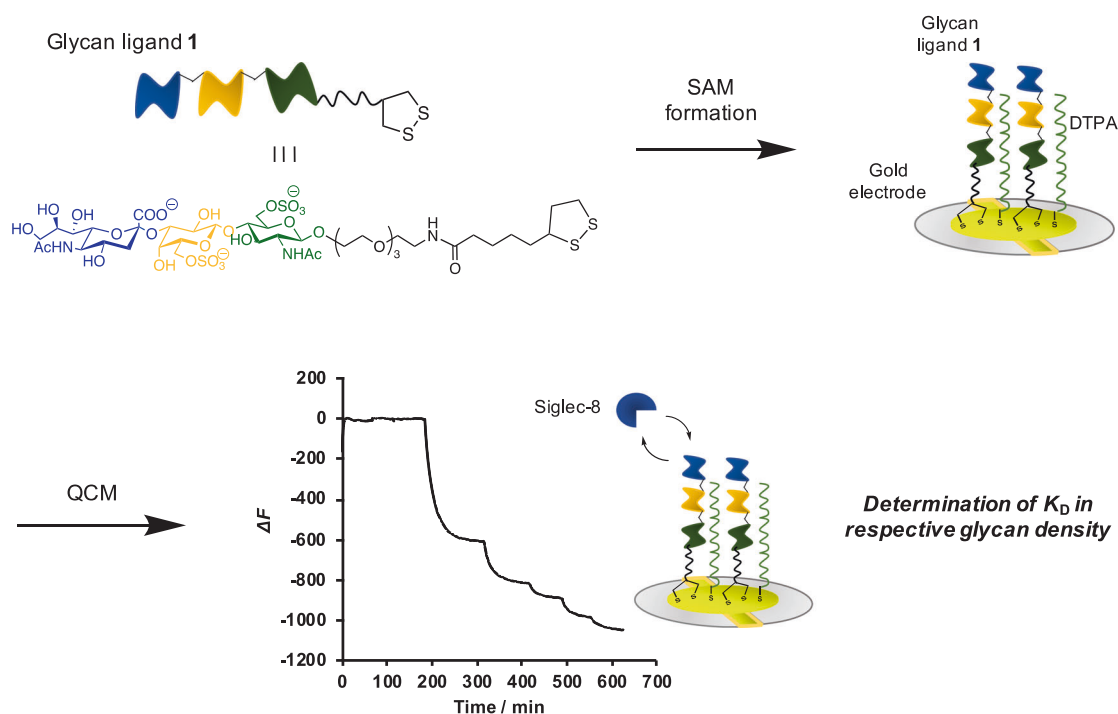
Fig. 1 Illustration of the current research strategy and methodology for determining the optimal glycan density for Siglec-8-glycan ligand interactions. Glycan ligand **1** was newly designed for immobilization on a gold electrode to investigate the Siglec-8 interactions. SAM surfaces with different glycan densities were prepared, and the apparent K_D values were measured with QCM to investigate the avidity of the glycan surface (see text for further explanation)

The second strategic step is to optimize the so-called "multivalent effect" of glycan ligands [7, 8]. It is well known that multivalently displaying glycan ligands, i.e., mimicking the cell surface "glycocalyx", provides dramatically higher apparent avidities toward glycan-recognizing proteins (lectins). Therefore, numerous studies have mimicked and reenacted the formation of this glycocluster with their glycan materials to improve their avidities with the targeted lectin [9, 10]. In addition, it is known that the three-dimensional arrangements of the lectin binding sites of glycan ligands are crucial to maximizing the multivalent effects [11]. When glycan ligands are densely oriented (highly coated), the accessibility of the glycan ligands to lectins is limited. On the other hand, when the glycan ligands are sparse (poorly coated), multivalent effects are ineffective in interacting with lectins, resulting in insufficient induction of biological responses. Therefore, we hypothesized that an optimal glycan density would also exist in the cases of Siglec-glycan interactions. However, to the best of our knowledge, there have been no reports describing the optimal densities for Siglec-glycan ligand interactions; the results could lead to the establishment of effective therapeutic methods due to the immune regulatory nature of Siglecs.

In this study, we aimed to determine the optimal glycan density for Siglec-8-glycan ligand interaction with quartz crystal microbalance (QCM) measurements (Fig. 1). QCM is a powerful tool with which to monitor biomolecular interactions in real time and obtain the thermodynamic dissociation constant (K_D) [12]. By constructing self-assembled monolayers (SAMs) with different glycan densities on the gold electrode surface of the QCM sensor cell, we estimated the avidities of the Siglec-8-glycan interactions at various glycan densities by determining the respective apparent K_D values. In this experimental system, the glycan density that showed the minimum K_D value was interpreted as the optimal glycan density for the Siglec-8-glycan ligand interaction.

Materials and methods/experimental procedures

Materials

α $(2 \rightarrow 3)$-Sialyltransferase from *Pasteurella multocida* (lot no. SLCC1110) and (±)-α-lipoic acid were purchased from Sigma–Aldrich (St. Louis, MO). Alkaline phosphatase from *E. coli* C75 was obtained from Takara Bio Co. (Shiga, Japan). Siglec-8 Fc chimera (lot no. TPX03201081, 50 μg) was obtained from Funakoshi Co. (Tokyo, Japan) and dissolved in PBS(-) (Dulbecco's phosphate-buffered saline, Invitrogen, 500 μL), which was purchased from FUJIFILM Wako Pure Chemical Co. (Osaka, Japan), before use. Other

chemical reagents were purchased from FUJIFILM Wako Pure Chemical Co. (Osaka, Japan) in guaranteed grade. All reagents were used without further purification unless otherwise noted. Gold mica substrates (Grade V4 Muscative Mica 25 mm × 25 mm, 5 nm Ti/10 nm Au) used in the atomic force microscopy (AFM) observation were purchased from Waki Company (Chiba, Japan).

Characterization procedures

^{1}H NMR spectra were recorded with a Bruker DPX-400 NMR spectrometer (Bruker Biospin, Rheinstetten, Germany) at 25 °C and 400 MHz. D_2O was used as the NMR solvent. Electrospray ionization mass spectrometry (ESI-MS) was conducted with a Thermo Fisher Scientific Exactive Plus Orbitrap Electrospray Ionization Mass Spectrometer (Thermo Fisher Scientific, Waltham, MA). The purity of the final compound was confirmed by reversed-phase chromatography performed with a RediSep Rf Gold C18 column (Teledyne ISCO Inc., Lincoln, NE).

Condensation with (±)-α-lipoic acid to prepare a Au-attachable Siglec-8 glycan ligand 1

Compound **2** (0.31 mg, 0.30 μmol), synthesized by following the procedure previously reported [6], was dissolved in methanol (180 μL). $Pd(OH)_2$-C (1.1 mg) was added to the solution and stirred at 25 °C for 3 h under H_2. The resulting mixture was filtered through filter paper to remove the catalyst. The solution was collected and evaporated to remove the excess solvent. To the resulting solid, a mixture of methanol (200 μL), ethanol (200 μL) and 4-(4,6-dimethoxy-1,3,5-triazin-2-yl)-4-methylmorpholinium chloride (DMT-MM, 0.21 mg, 0.84 μmol) was added. Next, (±)-α-lipoic acid (0.40 mg, 1.5 μmol) was added to the solution. After stirring at 25 °C under a dry atmosphere for 48 h, the reaction mixture was purified by column chromatography (C18, eluent; H_2O/MeOH = 1:0 to 0:1 v/v) to obtain **1** as an amorphous powder. The yield was 0.18 mg (51%). Here, we provide the ^{1}H NMR spectrum of **2** because **1** was not stable enough to maintain a single molecule structure in D_2O due to disulfide-mediated polymerization.

ESI-MS for **1** (*m/z*): [M + 2Na]$^-$ calcd. for $C_{41}H_{68}N_3Na_2O_{29}S_4$, 1240.2622; found, 1240.7018. [M+Na]$^{2-}$ calcd. for $C_{41}H_{68}N_3NaO_{29}S_4$, 608.6365; found, 608.6370.

^{1}H NMR for **2** (400 MHz, D_2O, 25 °C, ppm): δ 4.70 (d, 1H, $J_{1,2} = 8.0$ Hz, H-1), 4.66 (d, 1H, $J_{1',2'} = 7.6$ Hz, H-1'), 4.52-4.49 (m, 2H, H-6a, H-6b), 4.33–4.30 (m, 2H, H-6'a, H-6'b), 4.17–3.79 (m, 25H, H-2, H-3, H-3', H-3'', H-4, H-4', H-5'', H-5' H-6'', H-6'', H-8'', H-9''a, H-9''b, CH_2 of PEG×12), 3.74–3.56 (m, 6H, H-2', H-5, CH_2 of PEG×4) 2.32 (dd, 1H, $J = 4.8$, 12.8 Hz, H-3'' equatorial), 2.15 (s, 6H, CH_3 of Ac×6), 1.91 (t, 1H, 12.4 Hz, H-3'' axial).

Preparation of a SAM-coated gold substrate for AFM

For preparation of the glycan-containing SAM solution (200 μL), 3,3'-dithiodipropionic acid (DTPA; 4 mmol L^{-1}) was mixed with an aqueous solution of glycan ligand **1** (0.75 mmol L^{-1}). The respective amounts of glycan ligand **1** solution mixed to contain **1** were 1/500 or 1/2500 times less DTPA. Next, the gold-mica substrate (3 mm × 4 mm) was immersed in the respective SAM solutions and incubated at 4 °C for 14 h to form glycan-containing SAMs on the gold surface. In addition, the gold substrates were immersed in a DTPA solution (4 mmol L^{-1}, 200 μL) or in deionized water for preparation of the negative control. Afterward, the gold-mica substrates were washed with deionized water to remove the excess residues, dried and stored under vacuum before observation.
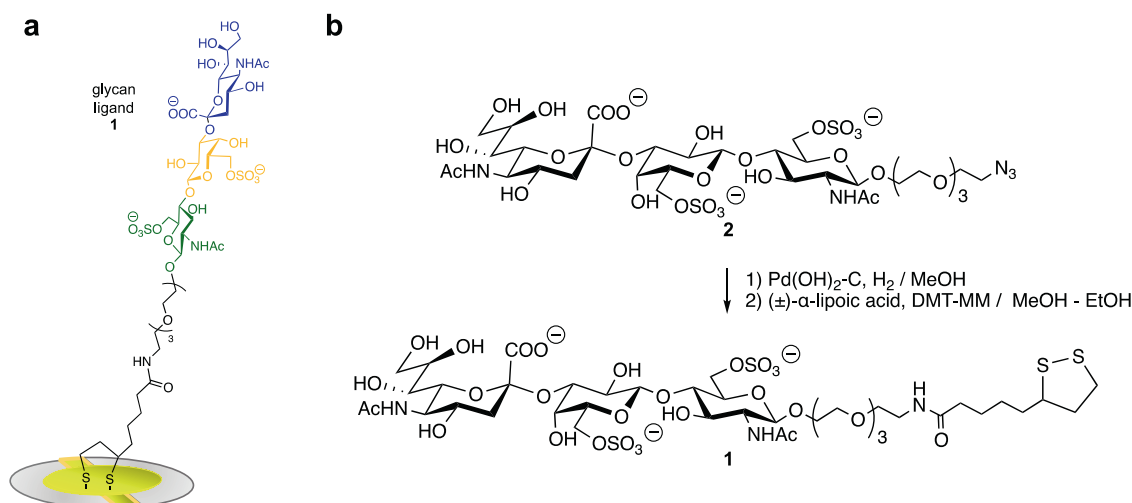
AFM measurements

AFM measurements were performed on a SAM-coated gold substrate by means of a Hitachi AFM 5300E system (Hitachi High-Tech Science Cooperation, Tokyo, Japan) using a silicon cantilever (SI-DF3, Hitachi High Tech Science, Tokyo, Japan) with a spring constant of 1.7 N m^{-1} in air at 25 °C. Tapping mode was used to map the topographical images of the SAM constructed on the gold substrate. The AFM height profiles were analyzed and quantified by Gwyddion (Version 2.58).

Preparation of a SAM-coated gold surface for QCM

First, the gold substrate was washed with 1% SDS solution (200 μL) and then rinsed with deionized water 3 times. Next, the gold substrate was washed with 2 μL of Piranha solution (30% hydrogen peroxide/98% sulfuric acid = 1:3) 4 times. Then, a SAM solution was prepared by dissolving **1** into DTPA solution (4 mmol L^{-1}). The respective amounts of **1** were dissolved at levels giving 500, 2500, and 5000 times more DTPA than **1**. Afterward, the gold electrode (gold surface area: 0.057 cm^2) was immersed in 200 μL of the SAM solution at 4 °C for 14 h to construct a SAM on the gold surface. The excess solution was removed and washed with 400 μL of potassium phosphate buffer (2 mmol L^{-1} containing 1 mmol L^{-1} NaCl) three times. Finally, the sensor cells were filled with 500 μL of potassium phosphate buffer (20 mmol L^{-1} containing 10 mmol L^{-1} NaCl).

QCM measurements

The QCM measurements were conducted at 25 °C with an Affinix Q4 batch measurement system (Initium, Tokyo, Japan). First, the SAM-coated sensor cells were attached

Fig. 2 Synthesis of glycan ligand **1**. **a** Glycan ligand **1** immobilized on a gold electrode. **b** Synthetic pathway for Siglec-8 glycan ligand **1** from compound **2** immobilized on a gold electrode for QCM measurements

and the frequency was allowed to stabilize. After stabilization, Siglec-8 solution ($0.1\ \mu g\ \mu L^{-1}$) was successively added to the cells as shown (Table S1), and the frequency changes were detected. After correcting these data, the K_D was determined by fitting the plots of ΔF versus the concentrations of Siglec-8 and using the Michaelis–Menten equation to obtain the regression line (1) with KaleidaGraph (version 4.5.3, Synergy Software, Reading, PA). ΔF_{max} is the maximal frequency shift for a fully saturated surface.

$$\Delta F = \frac{[\text{Siglec} - 8]\Delta F_{max}}{K_D + [\text{Siglec} - 8]} \tag{1}$$

Results and discussion

### Synthesis of a Siglec-8 glycan ligand containing (±)-α-lipoic acid as a thiol anchor

To elucidate the glycan density dependence in the interaction with Siglec-8 by QCM, a glycan ligand that forms SAMs on the surface of a gold electrode was synthesized. Here, we aimed to synthesize such a glycan ligand by modifying its aglycone structure to make it suitable for immobilization and formation of a SAM on the gold surface (Figs. 2, S1). As a starting material, we used a trisaccharide ligand consisting of sialyl *N*-acetyllactosamine bearing 6,6′-disulfate groups (**2**), which was reported as a Siglec-8 glycan ligand [3, 6]. Here, we chose **2** as a starting material, not only because it contains a Siglec-8 glycan ligand moiety but also because it includes an azido-terminated polyethylene glycol (PEG) linker. The PEG linker enhances the solubility in aqueous solution, which is ideal for QCM experiments in aqueous

conditions. Furthermore, we modified the aglycon structure of **2** using a (±)-α-lipoic acid moiety as an anchor for the gold substrate to enable immobilization of the glycan ligands on the gold surface via gold-sulfur bonds. This is because (±)-α-lipoic acid is widely used to form unified SAMs on gold surfaces by itself, and it undergoes condensation with amino groups derived from azido groups in **2** by catalytic reduction [13–18].

Starting from **2**, first, catalytic hydrogenation was conducted with Pd(OH)₂-C under H₂ in methanol to convert the terminal azido groups in the aglycon moiety into amine groups. Next, condensation of the converted amine group and (±)-α-lipoic acid was performed in a mixture of methanol and ethanol to synthesize **1**, which can be immobilized on a gold surface. In the condensation procedure with the amine from **2** and the carboxylic acid of (±)-α-lipoic acid, DMT-MM was used to give **1** in a good yield of 51%. The synthesis was confirmed by ESI-MS measurements (Fig. S2). Glycan ligand **1** does not completely dissolve in water, methanol, ethanol and tetrahydrofuran. Therefore, the addition of an ammonium solution dissolved **1** dissolve in water by suppressing the polymerization of (±)-α-lipoic acid through intermolecular disulfide bond formation. However, the added ammonia broadened the signals in the NMR spectra, making it difficult to precisely assign the NMR peaks of **1**.

Construction of a glycan ligand-displaying SAM on the gold-mica substrate

AFM was used to acquire topography information for the glycan ligand-containing SAM to confirm that the SAMs were constructed on the gold substrate (Figs. 3, S3). The bare gold surface was covered with small particles (height;
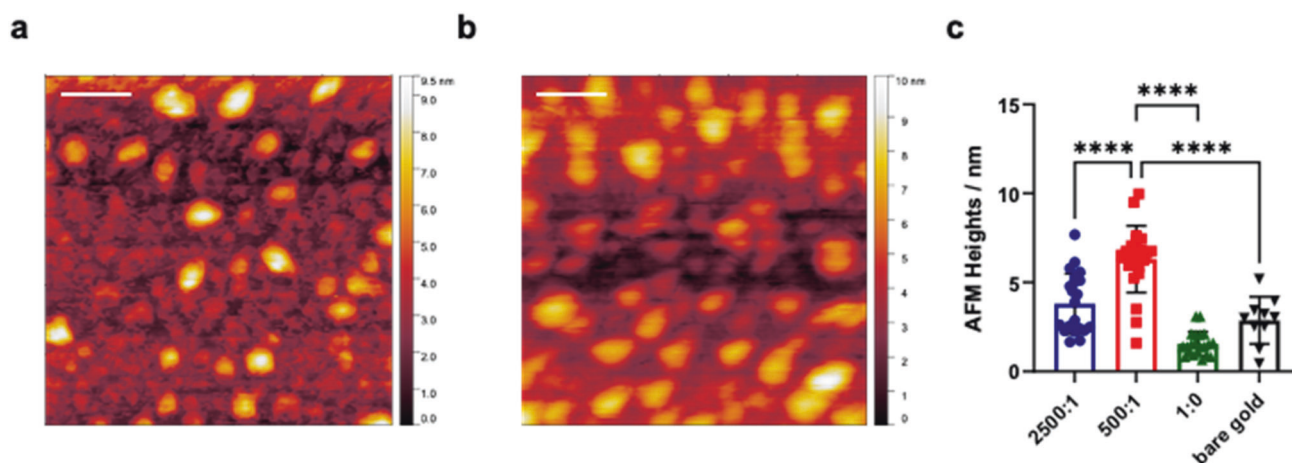
Fig. 3 AFM images (1 µm × 1 µm) of a SAM on a gold substrate with DTPA to glycan ligand **1** ratios of **a** 500:1 and **b** 2500:1. Scale bars, 200 nm. **c** Box plots of the height profiles for the small particles observed in the AFM images ($10 \leq n \leq 20$). Statistical significance was determined based on one-way ANOVA with Dunnett's multiple comparisons test (****$P < 0.0001$)

3.0 nm), which was attributed to small aggregates that were attached in the ambient air as previously reported (height; 2.3 nm), resulting in a height greater than that of the DTPA-coated gold surface [19]. Furthermore, the imaged SAMs appeared to have relatively small particles on the SAM-formed gold substrate, in contrast to the large crystalline structures observed for the previously reported SAMs formed with alkanethiols [20]. These small particles were attributed to decrystallization that occurred in air after removal from the alkanethiol solution [21, 22]. Both the bare gold surface and the SAMs were coated with small particles. However, the diameters of the particles for the former varied from 18 nm to 180 nm, while the diameters of the particles on the SAM surfaces were consistently ~100 nm (Fig. S4). Therefore, we considered that small particles with sizes of ~100 nm were peculiar topographical features of SAMs and only obtained height profiles from 100 nm particles for the height profiles of the SAMs (not for bare gold surfaces). Numerous studies have reported surface roughness to prove SAM formation; however, here, we only obtained the heights from 100 nm particles (which are considered SAMs) and did not include heights derived from other factors (i.e., contamination) that happen when obtaining only the roughness of the surface.

The particle heights observed for each surface were relatively uniform, ranging from 1.60 ± 0.66 nm (DTPA only, 1:0) to 3.04 ± 1.3 nm (bare gold surface), with the glycan coating increasing from 3.90 ± 1.7 nm (2500:1) to 6.53 ± 1.6 nm (500:1). Based on these results, it was confirmed that glycan SAMs with thicknesses of ~2–5 nm were constructed on the gold substrate surface (Fig. 3c). Furthermore, by increasing the ratio of **1** to DTPA in the SAM solution from 2500:1 to 500:1, the AFM heights increased from 3.90 ± 1.7 nm to 6.53 ± 1.6 nm. Since the

molecular length of **1** was roughly calculated as 3.0 nm, these stepwise increments in the height profiles (~3 nm) for the glycan-coated SAMs were attributed to the number of **1** molecules attached to the surface. This suggested that the number of **1** molecules on the SAM surface could be regulated by varying the ratio of DTPA to **1** in the 4 mM DTPA solution [23].

Dissociation constants to determine the optimal glycan density for the Siglec-8-glycan interaction

To determine the optimal glycan density for the interaction between Siglec-8 and the glycan, QCM measurements were conducted using SAMs with different glycan densities to quantitatively evaluate the avidities of the interactions with various glycan densities. We chose the optimal glycan density to be the density at which K_D calculated from the QCM measurements was at its minimum value in this experimental system. QCM sensorgrams were obtained from the QCM measurements (Fig. S5, Table S1). Nonspecific binding between Siglec-8 and DTPA was observed in each experimental system. This was attributed to the electrostatic interactions between positively charged Siglec-8 in a pH 7.4 solution (pI = 9.2) and the negatively charged carboxylate group of DTPA (Fig. S5a) [9]. On the other hand, Figure S5a suggests that nonspecific binding was saturated after the first injection. Therefore, the frequency changes after the second injection are thought to reflect the interaction of Siglec-8 and **1**, and K_D was calculated by excluding the first frequency change after injection of Siglec-8 to avoid the effects of nonspecific binding in calculating K_D. The K_D calculated here does not have a quantifiable meaning but is an indicator for evaluating the avidity of the Siglec-8-glycan interaction in this system.
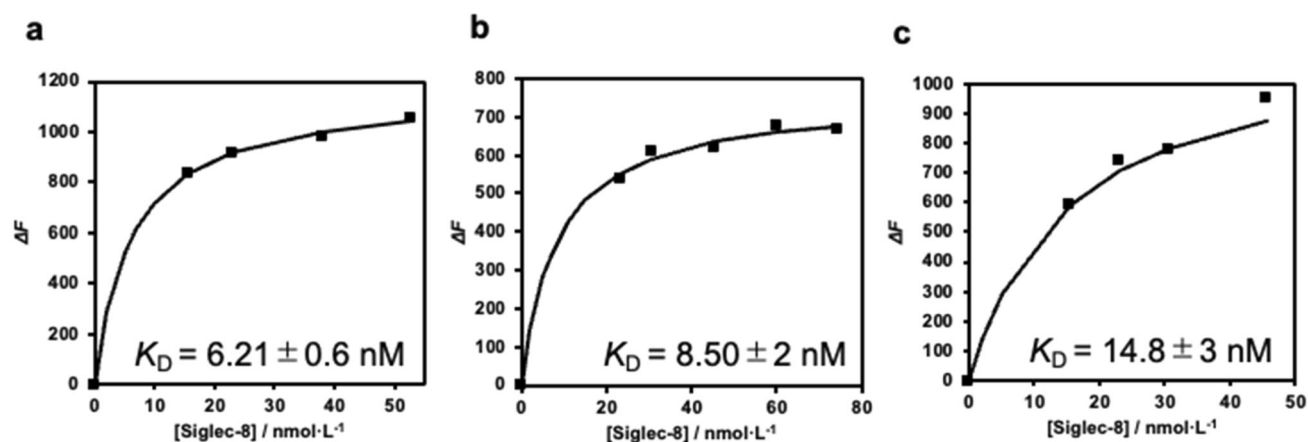
Fig. 4 Plots of ΔF obtained from QCM measurements versus [Siglec-8] among different glycan densities on the gold electrode (DTPA/glycan ligand **1**, **a** 2500:1, **b** 500:1, **c** 5000:1). The reported K_D values are the means ± SDs from separate fitting of plots obtained from technical replicates ($n = 3$)

The K_D calculated from the glycan density is shown in Fig. 4. These experiments showed that the apparent K_D values varied for the various glycan densities. When DTPA and **1** were coimmobilized on the gold electrode, the K_D obtained from the 2500:1 SAM showed the lowest K_D ($= 6.21$ nM) compared to the other SAMs with different glycan densities. We concluded that the 2500:1 SAM had the best glycan density for high-avidity binding with the Siglec-8-glycan interaction (Fig. 4a). The 500:1 SAM, which had a higher glycan density than the 2500:1 SAM, showed a higher K_D ($= 8.50$ nM) (Fig. 4b). This was possibly due to steric hindrance from the bulky glycan ligand **1**. For the Siglec-8-glycan interaction, the glycan ligand packed too densely on the surface prohibited the ligand from entering the receptor pocket of the Siglec-8 molecule and diminished recognition of the glycan ligand by Siglec-8. On the other hand, 5000:1 SAM, which had a lower glycan density than 2500:1, also showed a higher K_D ($= 14.8$ nM) (Fig. 4c). This can be explained by the decreasing multivalent effect. A multivalent effect requires a high local concentration of glycan ligands. Since the ligand molecules **1** in the 5000:1 SAM were separated from each other, it is thought that Siglec-8 was less likely to interact with **1** but also lost its chelation effect so that the Siglec-8 interaction was enthalpically disfavored [24, 25].

The glycan densities on the gold surface were calculated as shown in Table 1. It is known that thiolate groups, with densely packed structures of $(\sqrt{3} \times \sqrt{3})$R30° on the Au(111) surface, form a density of 4.62×10^6 molecules μm^{-2} [26]. Therefore, we assumed that the density of the thiolate groups in the SAMs was also 4.62×10^6 molecules μm^{-2}, and the density of **1** on the surface was estimated by multiplying the ratio of **1** to the total sulfur atoms on the gold surface by 4.62×10^6 molecules μm^{-2}. Based on this assumption, the optimal glycan density, the glycan density

Table 1 Estimated glycan densities on the gold electrode for QCM measurements

SAM solution[a]	Estimated glycan density on the gold electrode[b]
500:1 mixture	4.6×10^3 molecules μm^{-2}
2500:1 mixture	9.2×10^2 molecules μm^{-2}
5000:1 mixture	4.6×10^2 molecules μm^{-2}

[a]The solution mixed with DTPA/glycan ligand **1** at the indicated ratio was used to construct a SAM on the gold electrode surface

[b]Estimated glycan densities on the gold electrode from QCM measurements. The glycan density was calculated as described in the Results and Discussion section

in the 2500:1 SAM, was $\sim 9.2 \times 10^2$ [$= 4.62 \times 10^6/(2500 \times 2 + 1 \times 2)$] molecules μm^{-2} (Here, we note that in the calculation, the value "2" reflects two sulfur atoms in DTPA and glycan ligand **1**). Previously, it was reported that the frequency change observed via QCM was maximized at a glycan density of $\sim 9.2 \times 10^2$ molecules μm^{-2} in the lectin-glycan interaction of wheat germ agglutinin (WGA) and N-acetylglucosamine (GlcNAc), suggesting that the optimal glycan density for this interaction was near this range [23]. In addition, the glycan density of heparan sulfates, one of the sulfated glycan chains that resemble keratan sulfates in the human body, was reported as ~ 1200 molecules·μm^{-2} for effective interactions with WGA [27]. Although the lectin structure of WGA differs from that of Siglec-8, and it recognizes glycans differently, it is similar to Siglec-8 in that it recognizes sialic acid-containing glycoconjugates. Therefore, it is understandable that the optimal glycan density for the Siglec-8-glycan ligand **1** interaction calculated here was consistent with the ranges cited in these previous reports. To the best of our knowledge, however, there have been few reports of regulating the glycan density on the SAM surface at lower than 10^4–10^5 molecules μm^{-2}

to study of the interactions between lectins and glycan ligands, especially for studies on Siglecs [28]. Thus, further investigation on regulating the glycan density on the surface, especially at ~10^3 molecules μm^{-2}, might provide a better understanding of the avidity or specificity of Siglec-glycan ligand interactions required to induce the immunological response. For Siglec-8, this suggests that the development of glycan materials in which the glycans are decorated with an appropriate density (~9.2×10^2 molecules μm^{-2}) would improve the avidity between Siglec-8 and the glycan materials and enable efficient induction of immune responses involving Siglec-8 [2].

Conclusion

We developed the new Siglec-8 glycan ligand **1** and constructed a SAM of ligand **1** on the gold electrode surface of a QCM sensor to quantitatively evaluate the effect of glycan density on the avidity of the Siglec-8 interaction by calculating the apparent K_D. As a result, we found for the first time that the avidity of the interaction has a glycan density dependence and suggested that the glycan density for the Siglec-8-glycan interaction that maximizes the avidity is ~9.2×10^2 molecules$\cdot\mu m^{-2}$. Considering this estimate, glycan materials decorated with a glycan density of ~9.2×10^2 molecules μm^{-2} may be effective in regulating the immune response of Siglec-8. Further investigation is required to elucidate whether the avidity of the Siglec-glycan ligand interaction varies with the glycan density, even with other Siglecs. In addition, it is important to synthesize glycan materials that are decorated with the optimal density to efficiently and selectively induce immune responses via Siglec-glycan ligand interactions. The development of these glycan materials may lead to new methods to regulate Siglec-involved immune responses and contribute to clinical treatments of various diseases.

Compliance with ethical standards

Conflict of interest The authors declare no competing interests.

Publisher's note Springer Nature remains neutral with regard to jurisdictional claims in published maps and institutional affiliations.

References

1. Duan S, Paulson JC. Siglecs as immune cell checkpoints in disease. Annu Rev Immunol. 2020;38:365–95.

2. Kiwamoto T, Kawasaki T, Paulson JC, Bochner BS. Siglec-8 as a drugable target to treat eosinophil and mast cell-associated conditions. Pharm Ther. 2012;135:327–36.

3. Pröpster JM, Yang F, Rabbani S, Ernst B, Allain FHT, Schubert M. Structural basis for sulfation-dependent self-glycan recognition by the human immune-inhibitory receptor Siglec-8. Proc Natl Acad Sci. 2016;113:E4170–9.

4. Gonzalez-Gill A, Porell RN, Fernandes SM, Wei Y, Yu H, Carroll DJ, et al. Siaylated keratan sulfate proteoglycans are Siglec-8 ligands in human airways. Glycobiology. 2018;28:786–801.

5. Mattox DE, Bailey-Kellog C. Comprehensive analysis of lectin-glycan interactions reveals determinants of lectin specificity. PloS Comput Biol. 2021;17:e1009470.

6. Yuge S, Tateishi A, Numata K, Ohmae M. Chemoenzymatic synthesis of sialyl sulfo-oligosaccharides as potent Silec-8 ligands via transglycosylation catalyzed by keratanase II. Biomacromolecules. 2022;23:316–25.

7. Lee RT, Lee YC. Affinity enhancement by multivalent lectin-carbohydrate interaction. Glycoconj J. 2000;17:543–51.

8. Dam TK, Brewer CF. Effects of clustered epitopes in multivalent ligand-receptor interactions. Biochemistry. 2008;47:8470–6.

9. Hudson SA, Bovin NV, Schnaar RL, Crocker PR, Bochner BS. Eosinophil-selective binding and proapoptotic effect in vitro of a synthetic siglec-8 ligand, polymeric 6'-sulfated sialyl lewis X. J Pharm Exp Ther. 2009;399:608–12.

10. Duan S, Arlian BM, Nycholat CM, Wei Y, Tateno H, Smith SA, et al. Nanoparticles displaying allergen and siglec-8 ligands suppress IgE-FcεRI -mediated anaphylaxis and desensitize mast cells to subsequent antigen challenge. J Immunol. 2021;206:2290–300.

11. Dam TK, Brewer CF. Maintenance of cell surface glycan density by lectin-glycan interactions: a homeostatic and innate immune regulatory mechanism. Glycobiology. 2010;20:1061–4.

12. Sota H, Yoshimine H, Whittier RF, Gotoh M, Shinohara Y, Hasegawa Y, et al. A versatile plannar QCM-based sensor design for nonlabeling biomolecule detection. Ann Chem. 2002;74:3592–8.

13. Miura Y, Kimura S. Formation of oriented helical peptide layers on a gold surface due to the self-assembling. Langmuir. 1998;14:6935–40.

14. Hang Y, Noguchi H, Sakaguchi K, Uosaki K. Formation process and solvent-dependent structure of a polyproline self-assembled monolayer on a gold surface. Langmuir. 2011;27:11951–7.

15. Kunishima M, Kawachi C, Iwasaki F, Terao K, Tani S. Synthesis and characterization of 4-(4,6-dimethoxy-1,3,5-triazin2-yl)-4-methylmorpholinium chloride. Tetrahedron Lett. 1999;40:5327–30.

16. Kunishima M, Kawachi C, Morita J, Terao K, Iwasaki F, Tani S. 4-(4,6-Dimethoxy-1,3,5-triazin-2-yl)-4-methyl-morpholinium

chloride: an efficient condensing agent leading to the formation of amides and esters. Tetrahedron. 1999;55:13159–70.

17. Kunishima M, Kawachi C, Hioki K, Terao K, Tani S. Formation of carboxyamides by direct condensation of carboxylic acids and amines in alcohols using a new alcohol- and water- soluble condensing agent: DMT-MM. Tetrahedron. 2001;57:1551–8.

18. Tomabechi Y, Katoh T, Kunishima M, Inazu T, Yamamoto K. Chemo-enzymatic synthesis of a glycosylated peptide containing a complex N-glycan based on unprotected oligosaccharides by using DMT-MM and Endo-M. Glycoconj J. 2017;34:481–7.

19. Turetta N, Sedona F, Liscio A, Sambi M, Samori P. Au(111) surface contamination in ambient conditions: unravelling the dynamics of the work function in air. Adv Mater Interfaces 2021;8:2100068.

20. Ulman A. Formation and structure of self-assembled monolayers. Chem Rev. 1996;96:1533–54.

21. Lienemann M, Paananen A, Boer H, Fuente JM, García I, Penadés S, et al. Characterization of the wheat germ agglutinin binding to self-assembled monolayers of neoglycoconjugates by AFM and SPR. Glycobiology. 2009;19:633–43.

22. Yang G, Amro NA, Starkewolfe ZB, Liu GY. Molecular-level approach to inhibit degradations of alkanethiol self-assembled monolayers in aqueous media. Langmuir. 2004;20:3995–4003.

23. Wangchareansak T, sangma C, Ngernmeesri P, Thitithanyanont A, Lieberzeit PA. Self-assembled glucosamine monolayers as biomimetic receptors for detecting WGA lectin and influenza virus with a quartz crystal microbalance. Anal Bioanal Chem. 2013;405:6471–8.

24. Böhmer VI, Szymanski W, Feringa BL, Elsinga PH. Multivalent probes in molecular imaging: reality of future? Trends Mol Med. 2021;27:379–93.

25. Lenza MP, Atxabal U, Nycholat C, Oyenarte I, Franconetti A, Quintana JI, et al. Structures of the inhibitory receptor Siglec-8 In Complex With A High-affinity SialOSIDE ANALOGUE and a therapeutic antibody. JACS Au. 2023;3:204–15.

26. Sawaguchi T, Sato Y, Mizutani F. In situ STM imaging of individual molecules in two-component self-assembled monolayers of 3-mercaptopropionic acid and 1-decanethiol on Au(111). J Electroanal Chem. 2001;496:50–60.

27. Danzberger J, Donovan M, Rankl C, Zhu R, Vicic S, Baltenneck C, et al. Glycan distribution and density in native skin's stratum corneum. Ski Res Technol. 2018;24:450–8.

28. Hushegyi A, Bertok T, Damborsky P, Katrlik J, Tkac J. An ultrasensitive impedimetric glycan biosensor with controlled glycan density for detection of lectins and influenza hemagglutinins. Chem Commun. 2015;51:7474–7.